Journal of Colloid and Interface Science 482 (2016) 73–80

Contents lists available at ScienceDirect

Journal of Colloid and Interface Science

journal homepage: www.elsevier.com/locate/jcis

Neuron-like gold-palladium alloy nanostructures: Rapid synthesis and applications in electrocatalysis and surface-enhanced Raman scattering

Shan-Shan Li, Pei Song, Ai-Jun Wang, Jiu-Ju Feng *

College of Chemistry and Life Science, College of Geography and Environmental Science, Zhejiang Normal University, Jinhua 321004, China

GRAPHICAL ABSTRACT

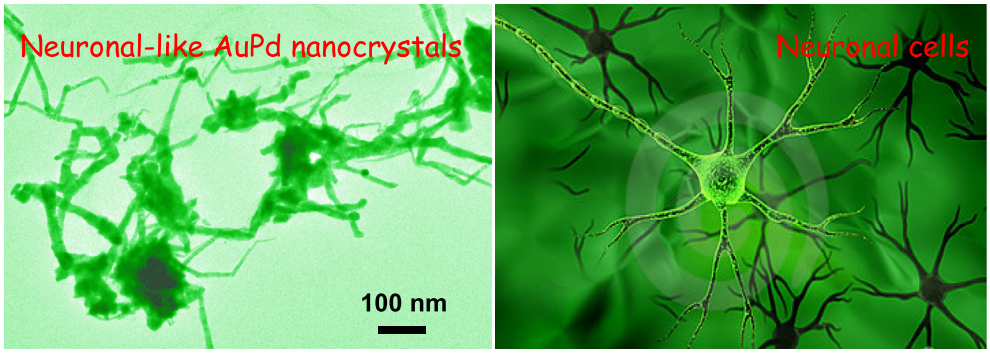

ARTICLE INFO

Article history:
Received 19 June 2016
Revised 26 July 2016
Available online 28 July 2016

Keywords:
Neuron-like nanostructures
Bimetallic alloy
N-methylimidazole
Ethanol oxidation reaction
Surface-enhanced Raman scattering

ABSTRACT

Neuron-like gold-palladium (AuPd) alloy nanostructures were synthesized by simultaneous reduction of $AuCl_4^-$ and $PdCl_4^{2-}$ with ascorbic acid, using *N*-methylimidazole as the structure-director and stabilizing agent. The synthesis method was simple and seedless, without any template or polymer. The architectures strongly depended on the concentration of *N*-methylimidazole, reaction temperature and time, and hence the formation mechanism was described in detail. The as-obtained architectures exhibited superior electrocatalytic activity for ethanol oxidation and surface-enhanced Raman scattering (SERS) responses, owing to their unique nanostructures with high density of steps, edges, and corners on their branches, along with the synergetic functions between Au and Pd.

1. Introduction

Direct alcohol fuel cells (DAFCs) were known as the promising power source instead of fossil fuel, due to the undoubted advantages of reproducible and environmental-friendly property [1]. Among these alcohols, ethanol had received more interests with the advantages of green, low cost and easy availability [2]. Nowadays, it is still urgent to develop efficient catalysts for DAFCs.

Furthermore, the discovery of surface-enhanced Raman scattering (SERS) has a great influence on the analytical chemistry and spectroscopy, because the inherently low response sensitivity is no more an obstacle for Raman spectroscopy [3,4]. The SERS effects make Raman spectroscopy as a valid in-situ diagnostic tool to determine the orientation of surface species and detailed structure information in electrochemistry, environment, biomedical engineering, and public security [4–7].

Until now, noble metal nanomaterials have attracted widespread attention owing to their fascinating physical and chemical properties, which are remarkably associated with the shape, size,

* Corresponding author.
E-mail address: jjfeng@zjnu.cn (J.-J. Feng).

http://dx.doi.org/10.1016/j.jcis.2016.07.073
0021-9797/

composition, and crystal structure [8], as well as their broad applications in catalysis, plasmonics, electronics, SERS, and biomedicine [9,10]. Thus, a variety of noble metal nanomaterials with different shapes were fabricated, such as cubes [11], plates [12], rods [13], wires [14], and prisms [10].

Especially, branched nanostructures with rough surfaces can be well used in surface-sensitive fields (e.g. SERS and catalysis) [15–17]. The enhanced SERS effects are attributed to the existence of many steps, edges and corners served as hot spots for large electric-field enhancement [17]. Besides, the existence of steps, edges, and corners in high densities provide more active sites, which are benefit for the catalytic reaction [18].

Notably, bimetallic alloy nanostructures often have better physicochemical properties than monometallic counterparts [19,20]. Recently, there are many bimetallic nanostructures prepared such as the highly branched concave Au/Pd bimetallic nanocrystals with good catalytic activity and highly efficient SERS from rod shaped Au/Pd seeds [17], rhombic dodecahedral Au-Pd alloy with improved SERS and efficient catalytic activity in the presence of cetyltrimethylammonium chloride (CTAC) [21], and Au@Pd core-shell nanocrystals with enhanced SERS and catalytic activity [22]. However, the above methods suffer from complicated reaction steps and time-consuming.

Herein, a simple one-pot aqueous approach was developed to synthesize neuron-like AuPd alloy nanostructures with the assistance of *N*-methylimidazole. The catalytic activity of the as-obtained nanocrystals was examined by using ethanol oxidation reaction (EOR) as the model system, and their SERS activity was also investigated by using malachite green as Raman probe.

2. Experimental

2.1. Preparation of neuron-like AuPd alloy nanostructures

For typical synthesis of neuron-like AuPd alloy nanostructures, 100 μL of 24.3 mM $HAuCl_4$, 25 μL of 100 mM H_2PdCl_4, and 20 μL of *N*-methylimidazole were dissolved into 8 mL of water. Subsequently, 2 mL of the freshly-prepared ascorbic acid (AA, 0.1 M) was dropwise added under magnetic stirring. Then, the mixed solution was kept in a 60 °C water bath for 10 min under stirring. The resulting precipitates were centrifuged and washed thoroughly with water and ethanol, and finally dried for further use.

Control experiments were conducted for preparation of individual Au (or Pd) nanoparticles by only using the precursor of $HAuCl_4$ (or H_2PdCl_4), and other AuPd products by varying the concentration of *N*-methylimidazole, reaction temperature and time, while the other experimental conditions were remained unchanged.

More information regarding chemical materials, characterization, electrocatalytic performances and SERS measurements is listed in Supporting Information (SI).

3. Results and discussion

3.1. Characterization of neuron-like AuPd alloy nanostructures

As illustrated by transmission electron microscopy (TEM) images (Fig. 1A and B), the typical product contains many neuron-like nanostructures with rough surfaces which are composed by neuronal cell-like nanoparticles and nerve fiber-like nanowires with the average diameter of 15 nm. There are lots of tips and edges decorated on the neuron-like nanostructures, which act as highly catalytic active sites for small reactants [17,23].

High-resolution TEM images (Fig. 1C and D) of the above nerve fibers provide more information regarding the crystalline characteristics of the neuron-like structures. There are many well-resolved fringe lattices with the *d*-spacing distance of 0.23 nm, corresponding to the (111) crystal planes of the face centered cubic (*fcc*) AuPd alloy [21]. This observation is similar to that of AuPd alloy in the previous literature [24]. As revealed by the associated selective area electron diffraction (SAED) pattern, the bright rings are well indexed to the (111), (200), (220) and (311) planes from inside to outside, showing the good crystallinity of the as-prepared neuron-like AuPd nanostructures (inset in Fig. 1B).

The high-angle annular dark-field scanning transmission electron microscopy (HAADF-STEM) images (Fig. 2A) further clearly display the neuron-like structures in this work. Importantly, the elemental mapping images (Fig. 2B–D) clearly reveal the uniform distribution of Au and Pd elements in the neuron-like AuPd nanostructures, as also supported by the cross-sectional line profiles of neuron-like AuPd nanostructures. It reveals the homogenous distribution of Au and Pd elements in the typical neuron-like AuPd structures, as seen in Fig. 3A. These observations demonstrate the formation of the AuPd alloy.

Fig. 3B shows the X-ray diffraction (XRD) patterns of neuron-like AuPd alloy nanostructures (curve a), using individual Au (curve b) and Pd (curve c) nanoparticles as the referenced materials. There are four well-defined diffraction peaks emerged at around 38.61°, 45.00°, 65.48°, and 78.58°, which correspond to the (111), (200), (220), and (311) planes of the *fcc* AuPd [25]. It is found that the diffraction peaks of neuron-like AuPd nanostructures coincidently appear between home-made pure Au nanoparticles and Pd nanoparticles, indicating the formation of AuPd alloy [26,27].

X-ray photoelectron spectroscopy (XPS) analysis was conducted to further examine the valence state and composition of neuron-like AuPd nanostructures. Fig. 4 shows the high-resolution Au 4f and Pd 3d XPS spectra of neuron-like AuPd alloy nanostructures. As seen in Fig. 4A, the Au $4f_{7/2}$ and Au $4f_{5/2}$ peaks show up at 83.88 and 87.53 eV, respectively, which are well ascribed to metallic Au^0 species, indicating the effective reduction of $HAuCl_4$ by AA [28,29]. However, the Pd 3d spectrum can be divided into two pairs of asymmetric peaks (Fig. 4B), suggesting the coexistence of Pd^0 and Pd^{2+} species. The binding energy peaks of Pd $3d_{5/2}$ at 335.31 eV and Pd $3d_{3/2}$ at 340.61 eV are indexed to Pd^0, while the binding energy peaks at 338.06 and 343.30 eV are originated from Pd^{2+} species [23,27]. By comparing the peak intensities of the oxidation with the reduction states, it is found that metallic Pd^0 and Au^0 are the main species in neuron-like AuPd nanostructures. Furthermore, the metal proportion of Au to Pd is calculated to be 17:83, according to the XPS data.

3.2. Formation mechanism

To illustrate the formation mechanism of neuron-like AuPd nanostructures, a series of control experiments have been carried out. Fig. 5 firstly shows the key role of the concentration of *N*-methylimidazole in the formation of neuron-like nanostructures. The absence of *N*-methylimidazole induces the formation of inhomogeneous nanoparticles (Fig. 5A). Some dendrites show up on the nanoparticle surface in the case of insufficient *N*-methylimidazole (Fig. 5B), and well-defined neuron-like AuPd nanostructures appear by using 25 mM *N*-methylimidazole in the standard process (Fig. 1). Alternatively, excessive *N*-methylimidazole causes the severe aggregation of the newly-formed thin nerve fibers (Fig. 5C and D).

Meanwhile, the reaction temperature has significant influence on the formation of neuron-like nanostructures. As illustrated in Fig. 6A, numerous dendrite-like nanoparticles are formed at low temperature, owing to the slow reduction rate of AA [30], and only a few Au-Pd seeds are formed at the early stage. Afterwards, newly-generated Au-Pd nuclei adsorb on the surface of the Au-Pd seeds and undergo epitaxial growth. When the reduction process